Structural and hemodynamic properties of ocular vasculature in axial myopia

Zhao M[1], Lam AKC[1,2], Cheong AMY[1,2]

1 Centre for Myopia Research, School of Optometry, Faculty of Health and Social Science, The Hong Kong Polytechnic University, Hung Hom, Kowloon, Hong Kong, China

2 Centre for Eye and Vision Research, Hong Kong, China

*Correspondence to:

Allen MY Cheong

Mailing address: Centre for Myopia Research, School of Optometry, Faculty of Health and Social Science, The Hong Kong Polytechnic University, Hung Hom, Kowloon, Hong Kong, China

E-mail: allen.my.cheong@polyu.edu.hk

Abstract

The high prevalence of myopia has become a global concern, especially in East and Southeast Asia. Alarmingly, prevalence of high myopia is increasing. Mechanical stretching caused by excessive eyeball elongation leads to various anatomical changes in the fundus. This stretching force may also lead to the development of vascular abnormalities, which tend to be subtle and easily overlooked. A healthy ocular vasculature is a prerequisite of adequate oxygen supply for normal retinal functions. This review summarizes previous findings on structural and hemodynamic aspects of myopia-related vascular changes.

Background

Myopia is a common vision disorder which has raised great global concern. By 2050, almost half of the world's population (49.8%) are predicted to suffer with myopia, of these approximately 10% would have high myopia.[1] The upsurge of myopia is especially alarming in East and Southeast Asia, where the prevalence of myopia in young adults (17-18 years) has reached 80-90% and that of high myopia is 10-20%.[2] East/Southeast Asian children manifest faster progression since myopia onset than white children [3], making them more susceptible to developing high myopia.

The International Myopia Institution has defined high myopia as a spherical equivalent (SE) refractive error ≤ -6.00 diopters (D) [4] and characterized pathological myopia by the presence of typical myopic lesions, such as chorioretinal atrophy and lacquer cracks.[5] Mechanical stretching is the predominant mechanism of myopia-related fundus changes. In addition, molecular alterations involving in scleral remodeling, active elongation of Bruch's membrane, inflammation, and vascular/atrophic changes might contribute the development of myopic maculopathies.[6] Myopia onset and development are influenced by an interaction of genetic and environmental factors. There have been many gene loci and variants identified.[7] Genetic factors were also associated with the development of myopic choroidal neovascularization.[8] Myopia onset might be better predicted if a genetic predictive model could leverage information from the genome-wide association study.[9] In general, myopia-induced structural changes that alter the fundus appearance, such as

staphyloma, dome-shaped macula, chorioretinal atrophy, are clearly evident and readily detectable, while, in contrast, vascular abnormalities tend to be more subtle and easily overlooked.

A healthy ocular vascular system is a prerequisite of adequate oxygen supply for normal retinal functions. Disrupted homeostasis of the ocular vasculature has been associated with many ocular abnormalities, including myopia. In experimental myopia using animal models, scleral hypoxia mediated eye growth, while anti-hypoxia drugs restricted myopia development.[10] Recent human genetic analyses also revealed enriched hypoxia-inducible factor 1-alpha (HIF-1α) signaling pathways in extremely high myopia (refraction≤-10.0D), illustrating the impact of scleral hypoxia on myopia development.[11] Therefore, understanding myopia-related vascular changes remains critical.

This review summarizes previous findings on myopia-related vascular changes from both structural and hemodynamic aspects. Structural changes among different groups of refractive errors in macular, peripapillary, and peripheral regions (i.e. retinal or choroidal areas other than macular and peripapillary) are discussed in sequence, while hemodynamic findings are categorized from retrobulbar, pulsative, peripapillary, and parafoveal perspectives. Through the integration of previous evidence, this review hopes to highlight future research directions, which would enhance the current understanding of myopia-related vascular changes.

Myopia-related structural changes in ocular vasculature

Macular perfusion

Retinal layers

Due to its non-invasive and efficient characteristics, optical coherence tomography angiography (OCTA) has become one of the most popular imaging modalities in the ophthalmic field. Interest has mainly focused on a 3 mm- or 6 mm-square area centered on the fovea. Most studies segmented the inner retina into the superficial and deep

capillary plexus (SCP and DCP, Figure 1),[12] although an intermediate/middle plexus (MCP) was occasionally suggested.[13] Vessel area density (VAD, %) and the area of the foveal avascular zone (FAZ) are the most common parameters in OCTA-related studies (Figure 2). Other parameters, such as vessel length density (VLD, mm^{-1}, Figure 2), flow index (arbitrary unit), and fractal dimension (arbitrary unit) are also frequently used. VAD (also referred to perfusion density) is defined as the proportion of white pixels (vascular area) over a particular retinal area. FAZ is the capillary-free region surrounding the fovea, which appears as the central no-flow area in the OCTA scan. VLD or skeleton density calculates the vessel length per unit area in the skeletonized images. Large vessels and small capillaries contribute to the VLD equally when neglecting vessel width, therefore, VLD may be more sensitive to perfusion defects in capillary level. Flow index, the average of decorrelation signal, combines the information of vessel area and flow velocity. Fractal dimension (FD) derived from the box-counting method is used to describe the complexity of vessel branching.

Although numerous studies have investigated the myopia-related changes of retinal perfusion, it remains difficult to reach a consensus on the effect of retinal stretching on retinal vasculature based on diverse findings. Table 1 summarizes the findings of recent reports. In the SCP (from inner limiting membrane to inner plexiform layer), most studies illustrated a damaged retinal vasculature in high myopia, manifesting as decreased VAD[14-23] and VLD[19,22,24], and reduced FD[14,25-27] as well as an enlarged FAZ.[20,21,28] However, a few studies observed that the VAD[29-32], flow index[29,31] and FAZ area[19,23] were comparable between high myopes and emmetropes/ low myopes. Surprisingly, one study[33] reported that the FAZ area tended to decrease with axial length (AL, coefficient of linear regression = -0.215, R^2 =0.046, p = 0.001), especially in high myopes (coefficient of linear regression = -0.359, R^2 =0.129, p = 0.009). Discrepancies were also found in the DCP, which generally extends from the inner plexiform to the outer plexiform layer. The deep VAD might be decreased,[14-18,20] unaffected,[21,22,30] or even increased[24,31] in high myopia (Table 1). Results of other parameters, including FAZ area,[23,28,33] flow index,[31] VLD[22,24] and FD[14,25-27] were also inconsistent across different studies.

The abovementioned discrepancies in myopia-related changes of retinal perfusion could be due to differences in the clinical characteristics of subjects and methods of measurements. The definition of high myopia varied among studies, with different cutoff values of SE (-5D[26], -6D[16,22,27]) and AL (26.5mm[14,16,21], 26mm[19,20], 25.5mm[17]). Myopia-related pathological changes were excluded in some studies (e.g. Sung, et al. [28] and Min, et al. [21]) but included in others (e.g. Mo, et al. [16] and Ye, et al. [34]). In addition, some studies partially excluded subjects with severe changes because these could interfere with OCTA imaging[22]. Longer AL and more myopic refractive status are associated with higher risks of pathological changes. As suggested by Mo, et al. [16], including pathological myopia would further decrease VAD compared with high myopia without pathological changes. With respect to measurements, the effect of ocular magnification leads to an inaccurate estimation of OCTA parameters, but it was only controlled in a few studies. According to Sampson, et al. [35], superficial VAD was overestimated (i.e. corrected/true VAD < uncorrected/measured VAD) for eyes with longer AL than the calibrated AL (e.g. 23.82 mm for RTVue) of the OCTA device, but underestimated for shorter eyes. The relative changes (i.e. after correction – before correction) of superficial VAD, induced by ocular magnification, ranged from -20% to +10% in the fovea and around -3% to +2% in the parafoveal area. Therefore, the VAD difference between high myopes and emmetropes could become less significant after correction.OCTA images of the deeper retinal layers (i.e. MCP and DCP) may also be affected by projection artifacts caused by superficial vessels. Zhu, et al. [24] reported the VAD and VLD of MCP and DCP, before and after removing the projections. In MCP, the insignificant difference of VAD between high myopes and emmetropes became significant after projection removal, while the difference in VLD changed in a reverse direction. Although the projection artifacts have remarkable effects on deeper VAD/VLD, simply suppressing all projections could also cause the signal loss of "real" vessels. Different sampling strategies and data analysis might be another source of variance, as some studies included both eyes,[25,30] while others only included one [20,32]. As subjects with anisometropia were commonly excluded,[25] it is very likely that measurements of two eyes from the same subjects were highly correlated. Hence, study cohorts tend to be overrepresented and biased and group differences might appear more significant than in actuality[36]. Finally, age may also contribute to the discrepancy since both VAD[37] and FAZ area[38] are age-dependent. Most studies in Table 1 recruited adults

with a mean age between 20 to 40 years, but the mix of younger [20,29] (under 20 years) and senior[14,21,39] (over 40 years) subjects could complicate the overall analysis.

High myopia is a strong risk factor for glaucoma. However, diagnosis of glaucoma in highly myopic eyes can be difficult due to the similar optic disc appearance and RNFL thinning. Macular perfusion has been suggested to detect early glaucoma in high myopia. Lee, et al. [40] compared the diagnostic ability of OCT and OCTA parameters in detecting glaucoma. They found that the inferior macular VLD ratio (i.e. inferior outer VLD/average inner VLD, 6mm-ETDRS grid) showed better diagnostic accuracy for glaucoma in high myopes than using conventional OCT measures such as peripapillary RNFL thickness and macular ganglion cell-inner plexiform layer.

Interestingly, recent studies have suggested that cilioretinal arteries potentially improved retinal perfusion[41] and protected against myopic macular degeneration[42] in high myopes. Highly-myopic eyes with cilioretinal arteries displayed a higher VAD and FD in both SCP and DCP, a smaller FAZ, and better visual acuity than those without. However, these differences were insignificant when the AL exceeded 30 mm.[41] Further studies are needed to examine the protective mechanism of cilioretinal arteries on retinal vasculature.

CHOROIDAL LAYERS

Apart from mapping the choroidal thickness profile, optical coherence tomography (OCT) B-scan is also useful to analyze the choroidal vascularity index (CVI), which is defined as the ratio of vascular area relative to the total choroidal area (Figure 3). Gupta, et al. [43] extracted the details of the choroidal stroma and vessels from binarized OCT B-scans. Compared with emmetropes, highly myopic individuals showed reduced areas of choroid vessels and stroma, as well as an increased CVI. However, adopting the same method, Alshareef, et al. [44], detected no significant difference between myopia and emmetropia in either the vascular area or CVI. This discrepancy might be explained by the smaller sample size and less myopic eyes in Alshareef, et al. [44] (60 eyes; mean AL: 26.3mm), comparing with Gupta, et al. [43] (515 eyes; mean AL: 27.3mm). Agrawal, et al. [45] suggested that CVI might be a better biomarker to monitor choroidal changes, as it was influenced

by fewer physiological factors compared with subfoveal choroidal thickness. A single B-scan passing through the fovea can represent the choroidal vascularity of the whole posterior pole in healthy subjects,[46] presenting the overall vascular distribution without details of the sublayer. In addition, the choriocapillaris might be misclassified as stroma during the binarization, as they have similar contrast levels in the B-scan, so the CVI mainly reflects the vascular changes of large choroidal vessels.

Unlike the extensive application and good performance of OCTA in the retinal vasculature, visualizing the choroidal vessels by OCTA remains challenging. The light beam is scattered by the overlayed retinal pigment epithelium (RPE) layer. The choroidal flow signals significantly attenuate in eyes with intact RPE even with long-wavelength swept-source OCT (SS-OCT).[47] Zhang, et al. [48] proposed a method to compensate for the shadowing effect induced by the RPE and Bruch membrane complex in the choriocapillaris angiogram, but this method was only tested in limited samples and might not be effective in cases with highly varied RPE reflectivity (e.g. RPE detachment, macular edema). Another impediment is the lateral/transverse resolution. Human choriocapillaris in the posterior pole has an inter-capillary distance of 5-20 μm,[49] which is similar to the lateral resolution of most commercially-available OCTA devices (6-20 μm).[50] Thus, visualizing the details of choriocapillaris is still very challenging.

Despite the limitations in image quality, OCTA manifestations of myopic choriocapillaris have been studied qualitatively and quantitatively. Qualitatively, Wong, et al. [51] and Sayanagi, et al. [52] categorized the choriocapillaris flows of highly myopic eyes. A complete loss of choriocapillaris and large vessels was found in areas with patchy atrophy, while a partial loss of choriocapillaris was observed in areas with lacquer cracks. Diffuse atrophy exhibited as a reduced density of choroidal vessels. Quantitatively, some studies reported that the perfusion area (mm^2)[39,53], VAD[29], and flow index[29] of choriocapillaris were similar in high myopes and emmetropic controls. In contrast, Mo, et al. [16] found a reduced choriocapillaris VAD in high myopes and pathologic myopes compared with emmetropes. The discrepancy between Wang, et al. [29] and Mo, et al. [16] was likely attributable to the age of the subjects (mean age: Mo et al. vs. Wang et al., 38 vs. 16 years). Rather than quantifying choriocapillaris perfusion directly, Spaide [54] proposed an alternative strategy,

namely flow voids, to analyze the areas without flow signal in the choriocapillaris angiogram. This method has been extensively utilized in later studies.[14,22,55,56] Al-Sheikh, et al. [14] reported an increased total and average flow void area along with a reduced number of flow voids in high myopes compared with healthy controls. Su, et al. [22] detected a higher percentage of flow voids in high myopes and these changes were present in the absence of pathological myopia. Compared with Al-Sheikh, et al. [14] (3 × 3 mm) and Su, et al. [22] (6 × 6 mm), Mastropasqua, et al. [57] analyzed the flow voids in a wider area, which was covered by a 6mm-circle center on the fovea and three 4.5mm-circles tangential to the macular circle from superior, inferior and temporal sides. The total flow void area of macular and paramacular areas were both increased in high myopes compared with emmetropic controls.

Choroidal thinning caused by axial elongation mainly affected Haller's and Sattler's layers rather than the small vessels.[58] A few attempts were made to analyze the large choroidal vessels in OCTA images. Maruko, et al. [59] attempted to observe large choroidal vessels indirectly through the projections on the sclera. Choroidal blood flow was visualized in 41 out of 92 highly myopic eyes (mean SE: -12.7 ± 5.2D) after placing the posterior segmentation line within the sclera. However, it was not visible in all 54 age-matched non-highly myopic eyes. The subfoveal choroidal thickness of highly myopic eyes with visible choroidal blood flow was significantly thinner than those in which the flow was not visible and non-high myopes (50.3 ± 42.2 vs. 100.3 ± 44.4 vs. 275 ± 89μm, respectively). This indirect method is feasible, but is only applicable for high myopes with an extremely thin choroid. Diaz, et al. [47] tested this approach on three OCTA devices with different light source wavelengths and reached a similar conclusion with Maruko, et al. [59]. The longer wavelength of swept-source OCT did not improve the imaging performance in eyes with intact RPE. A recent study described a novel technique to analyze the choroidal vessels quantitatively.[60] By correlating the OCTA image with structural OCT, the choroid was segmented into three layers: choriocapillaris (not used for analysis), Haller's layer, and Sattler's layer. The choroidal vessel density (CVD, similar to VAD), choroidal branch area (CBA, similar to VLD), and mean choroidal vessel width (=CVD/CBA) of Haller's and Sattler's layers were compared between high myopia (-8.0 D ≤ SE < -5.0 D) and extreme myopia (SE < -8.0 D). Participants with extreme myopia had thinner Haller's and Sattler's

layers, responding to the overall choroidal thinning. Only the CBA of Haller's layers was found to increase slightly in extreme myopia (9.95 ± 0.8 vs. 10.2 ± 0.7, p=0.018), which might be explained by diverse vascular branching patterns among individuals.

Peripapillary perfusion

RETINAL LAYERS

Fluorescein angiography (FA) cannot adequately image radial peripapillary capillaries (RPC).[61] In contrast, OCTA exhibits superior performance in viewing RPC, the capillary beds within the retinal nerve fiber layer (RNFL), and has been applied in many studies examining peripapillary retinal perfusion.

Extensive studies[16,20,28,32,62] have supported the presence of an impaired RPC perfusion in high myopes (Table 2). Pathological myopia was characterized by sparser RPC distribution than in high myopia and emmetropia in all tested regions,[16] while the differences between high myopia and emmetropia only appeared in some sectors.[16,32] AL[16,18,20,32,63] and area of peripapillary atrophy[20,62] both showed negative correlations with RPC density, but positive correlations were detected between SE[20], RNFL thickness,[20,32,62] and RPC density. Peripapillary intrachoroidal cavitation (PICC) is defined as an intrachoroidal hyporeflective cavity with a normal overlying retina in OCT scans. The existence of PICC further worsens RPC perfusion, [62,64] although the clinical significance of this phenomenon remains unknown.

A small number of studies[15,19,29,62] have broadened their research interests into the deeper retina to analyze the VAD of a peripapillary retinal layer extending 150 μm below the inner limiting membrane (ILM). Of these, only Chen, et al. [62] revealed a decreased VAD in high myopes compared with low myopes or emmetropes. In contrast, Fan, et al. [15] reported no difference among moderate and high myopes and emmetropes; Wen, et al. [19] showed no significant correlation between VAD and AL. Lee, et al. [65] calculated the VAD of a similar retinal layer (130 μm below the ILM) in 124 highly myopic eyes with primary open-angle glaucoma (POAG). They reported that the VAD displayed a similar topographical correlation with visual field defects as the RNFL thickness did, indicating

its usefulness in diagnosis of glaucoma, especially when segmentation errors occur in the RNFL profile. Use of full-layer retinal perfusion by Wang, et al. [29] revealed that the peripapillary retinal flow index and VAD were lower in high myopes compared to mild myopes and emmetropes.

CHOROIDAL LAYERS

Limited studies have examined choroidal perfusion in the peripapillary area. Wang, et al. [29] reported that the choroidal flow index and VAD did not vary among high, moderate, mild myopia, and emmetropia. In contrast, Mastropasqua, et al. [57] found increased peripapillary flow void areas in high myopes, which was greater than the flow void areas in macular and paramacular regions. Choroidal microvasculature dropout (MvD), defined as localized complete loss of choriocapillaris at the juxtapapillary area, was typical OCTA observation in glaucomatous eyes, which has been topographically associated with glaucomatous RNFL thinning.[63,66] The prevalence of choroidal MvD in myopic eyes with POAG was 47.6%[63] and 97.8%[66], respectively. Both studies stated that no MvD was detected in healthy myopic eyes. The higher prevalence reported in Na, et al. [66] might be attributable to more advanced myopia, with a mean AL of 28.38 mm, compared with Shin, et al. [63] (26.71 mm). Surprisingly, MvD-like defects located at the non-juxtapapillary area in healthy myopic eyes were detected by a recent study, although their clinical significance remains unclear.[67]

Peripheral perfusion

Compared with macular and peripapillary regions, peripheral perfusion has seldom been investigated in myopia.

Both FA and indocyanine green angiography (ICGA) may be utilized to visualize dynamic blood circulation. Kaneko, et al. [68] used ultra-widefield (approximately 200°) FA to detect vascular abnormalities in the far peripheral retina (the area anterior to the ampullae of the vortex veins) and speculated that peripheral avascularity might be a characteristic of highly myopic eyes, as 82.6% of eyes with high myopia presented an avascular region in the far peripheral retina, while only 4.8% of emmetropic eyes showed similar alteration.

Although peripheral avascularity was found in most of the high myopes, none showed retinal neovascularization.

Large choroidal vessels are better visualized with ICGA than FA, due to the slower rate of dye leakage from the choriocapillaris. Quaranta, et al. [69] and Moriyama, et al. [70] described the ICGA features of eyes with pathological myopia, both reporting that choroidal flush (i.e. filling of smaller choroidal vessels and choriocapillaris) was absent and that the number of large choroidal vessels tended to be reduced in highly myopic eyes compared with non-myopic eyes. Furthermore, in non-myopic controls, the posterior ciliary arteries entered the eye in the macular region, while the entry site was displaced to the midperiphery in more than half of the highly myopic eyes.[70] The choroidal venous blood normally exited the eyeball through the vortex veins located in the equator, but the outflow site could be near the optic disc or the macular in highly myopic eyes.[70] This posterior route of choroidal blood outflow was observed in 23.9% of highly myopic eyes, but in only 2.4% of non-myopic controls.[71] This myopia-induced alteration of the spatial distribution of vasculature might be due to significant stretching and deformity of the posterior sclera. However, the exploration of the topographic relationship of choroidal blood flow is limited by the two-dimensional display of the vasculature.

Use of wide-field OCTA achieved by the montage of multiple scans has increased in recent years and applied to myopia-related studies. However, as reported by Mastropasqua, et al. [57], the peripheral area of the OCTA montage was significantly affected by the shadow of eyelashes (even though the subjects were dilated) and image distortion, so only the near periphery (about 10.5 degrees around fovea) could be selected for quantitative analysis. In future, the application of wide-field OCTA will further increase with more advanced image processing.

Myopia-related hemodynamic changes in ocular vasculature

Retrobulbar blood flow

Color Doppler Ultrasonography (CDU) is commonly used to study the retrobulbar circulation (Figure 4) in various ocular conditions. Hemodynamic characteristics of the ophthalmic artery (OA), central retinal artery (CRA), and posterior ciliary arteries (PCA) have been extensively studied in myopic eyes. Similar to structural changes in ocular vasculature, mixed findings were reported in the retrobulbar blood flow of high myopes.

Several studies have revealed decreased CRA flow velocities[72-74] and elevated vascular resistance[73,75] were recorded in high myopes and impaired CRA hemodynamics were associated with increased severity of myopic degenerative changes,[76] in contrast, Galassi, et al. [77] did not detect any difference in CRA parameters between high myopes and non-myopic controls. Dimitrova, et al. [78] established a negative correlation ($r = -0.34$, $p = 0.013$) between AL and resistance index (RI), indicating longer eyes had lower vascular resistance. Their findings were contradictory to other studies,[73,75] which might be due to the characteristics of their subjects, who had a wide range of refractive errors (-22.0 to +4.3D) and age (23 to 78 years).

The findings with respect to PCA were also diverse. A slower PCA flow[72,74] and a higher RI[72,75] in high myopes were reported in some studies, while others[73,77] found no significant difference between high myopes and emmetropes in any PCA parameter. Dimitrova, et al. [78] identified a significant positive correlation between PCA velocities and SE, but the correlation between PCA velocity and AL was not significant. The challenge in measuring PCA might partially explain the diversity in the PCA findings. Individual PCA cannot be distinguished by the CDU, so the obtained waveforms actually represent the mass effect produced by a bundle of vessels.[79]

Benavente-Perez, et al. [73] examined the OA hemodynamics of high myopes with refractive errors between -9.4 to -5 D and found no difference when compared with emmetropes. Karczewicz and Modrzejewska [74] included patients whose myopia ranged from -2D to -25D, and only high myopes with a SE < -8D showed decreased mean velocity compared with emmetropes. Similarly, Galassi, et al. [77] observed slower OA velocities in high myopia with an AL over 27.5 mm. It seems that the association between high myopia and OA

hemodynamics only appears after the refractive error or axial length reaches a certain threshold. However, current evidence is too limited to draw a firm conclusion.

The fluctuating reproducibility of CDU parameters may partially contribute to the inconsistent CDU results mentioned above. Use of CDU is a complicated skill with a long learning curve. The reproducibility of CDU measurements is highly dependent on operators' skill and varies remarkably in reports. For example, CRA velocities had an intra-observer intraclass correlation coefficient from 0.53 to 0.80 and a coefficient of variation from 6.9% to 25.8% in healthy subjects.[79] The agreement and variation of PCA and OA measures were similar to those of CRA.

Pulsative volume change

IOP increases with heart contraction and gradually falls following heart relaxation. The rhythmic IOP changes during cardiac circles can be converted to volume changes by particular pressure-volume relation.[80] The pulsatile ocular blood flow (POBF, μL/min) indicates the summed arterial inflow. The maximum IOP change during the cardiac circle is defined as the pulse amplitude (OBFa, mmHg).

Several studies have investigated myopia-related changes in ocular pulsatile components. A negative correlation between AL and pulsatile components (e.g. OBFa and POBF) was observed in most studies.[73,81-85]. However, it might be inaccurate to conclude that myopia altered the pulsatile blood flow because of other plausible factors. According to Dastiridou, et al. [86], the OBFa was positively correlated with ocular rigidity, which decreased in longer eyes.[84] Therefore, the reduced OBFa in myopic eyes may simply be caused by the decreased rigidity. Berisha, et al. [83] also reported the relationship between AL and POBF, which appeared to be a consequence of different ocular volumes in hyperopic, emmetropic, and myopic eyes. Benavente-Perez, et al. [73] analyzed the interaction between retrobulbar and pulsatile blood flow and speculated that a lower pulse amplitude in longer eyes would not necessarily imply reduced retrobulbar flow velocities. The central retinal artery and pulsatile ocular blood flow may be influenced by each other and behave independently of the axial length.

Peripapillary hemodynamics

Except for retrobulbar vessels, peripapillary blood hemodynamics, such as vessel diameter, flow velocity, and oxygen saturation, may also suffer some changes in myopic eyes.

Shimada, et al. [87] used laser doppler velocimetry to measure the flow velocity and diameter of a major superotemporal or inferotemporal artery before its first branching. They found that highly myopic eyes had thinner arteries than those of mild myopes and emmetropes after correcting for ocular magnification effect. No difference in flow velocity was observed among the three groups. The blood flow volume (μL/min), calculated based on the simultaneous velocity and diameter measures, was found to decrease in high myopia. By using laser speckle flowgraphy, another parameter, mean blur rate, was introduced, which is a relative measure of blood velocity and correlated with the actual flow rate. This rate was reduced in eyes with myopic disc (i.e. being oval and temporally tilted with crescent peripapillary atrophy), but normal visual field. This study disclosed subtle damage to peripapillary circulation before the occurrence of visual field defects.

Since the number and branching pattern of large retinal vessels varies across individuals, between-group comparison based on individual vessels might not be appropriate. Therefore, Zheng, et al. [88] averaged the diameters of arterioles and venules within a 400-pixel circle (9.3μm/pixel) from the disc margin. High myopes had narrower arterioles and venules than healthy controls. Subgroup analysis revealed that high myopes with more advanced myopic retinopathy had narrower arterioles, but the difference in venous diameter was not significant between the two subgroups. La Spina, et al. [89] utilized the concept of equivalent width to summarize the central retinal artery/vein equivalent (CRAE/CRVE) based on individual vessel calibers, within a range of 1.5 to 2 disc diameters from the disc margin. They discovered decreased CRAE and CRVE in high myopes with and without pathological changes compared with emmetropic controls. Similar results were also reported by another large-scale study,[90] which selected blood vessels closer to the optic disc (0.5 to 1.0 disc diameter) for CRAE and CRVE measurement.

Of note, a cautious interpretation regarding any observed difference in vessel diameter is required because of the existence of pulse-related change during cardiac cycles. In 1994, Chen, et al. [91] synchronized an electrocardiogram with a retinal camera to image retinal vessels in eight different pulse points of a cardiac cycle. The maximum caliber changes of venules and arterioles during a cardiac cycle were 6.89μm (point 1/8 to 5/8, Table 1 in Chen, et al. [91]) and 3.73μm (point 1/8 to 3/8, Table 3 in Chen, et al. [91]), respectively. By using a similar method, Hao, et al. [92] observed a maximum caliber variation in venules of 4.2μm (point 2 to 6, Table 1 in Hao, et al. [92]) and in arterioles of 3.9μm (point 1 to 3, Table 1 in Hao, et al. [92]). In recent years, because of the significant improvement in the lateral resolution (1.6μm/pixel), adaptive optics retinal imaging offers a more precise way to measure vessel caliber. The ability to distinguish lumen from vessel wall makes it a better tool to monitor fundus vessels in physiological and pathological conditions.[93]

Oxygen saturation of retinal vessels can be estimated by comparing the light absorption of oxygenated and deoxygenated hemoglobin. A decreased arterial saturation and an unchanged venous saturation with increasing AL were commonly reported in previous studies,[88,94,95] while the alteration of oxygen consumption (i.e. difference between arterial and venous saturation) remains uncertain. Zheng, et al. [88] found lower oxygen consumption in highly myopic eyes, while Heitmar [94] and Lim, et al. [95] reported that it was not affected by axial elongation. Decrease oxygen saturation does not necessarily mean reduced blood supply. It may be caused by increased oxygen transportation between central retinal vessels or be just an uncorrected measurement error. [88]

Parafoveal hemodynamics

Evaluating parafoveal hemodynamics is difficult as the flow patterns of individual capillaries are highly heterogeneous.[96] Benavente-Perez, et al. [73] found that the blood volume and velocity of parafoveal capillaries were comparable in high myopes, low myopes, and emmetropes. Similarly, Li, et al. [26] and Qu, et al. [97] also reported that no significant difference was detected between high myopes and controls (low myopia or emmetropia) in parafoveal flow velocities. Based on the unchanged blood velocity and

volume[73], Li, et al. [26] speculated that the overall perfusion was maintained at the parafoveal region. Therefore, the decreased density of retinal microvasculature (i.e. FD of SCP and DCP) found in their study was likely caused by retinal stretching rather than capillary loss.

Parafoveal choroidal circulation of low myopes (mean SE: -3.80D) and emmetropes were compared by Benavente-Perez, et al. [98] At baseline (breathing room air), the choroidal blood velocity of myopes was 28% lower than that of emmetropes. After breathing CO_2-enriched air to induce stress on the choroidal circulation, the velocity of myopes increased to the baseline level of emmetropes, whereas the velocity of emmetropes did not show significant change. This study further confirmed that the choroid has some auto-regulatory capacity. Consistently, Samra, et al. [99] also suggested a decreased choroidal blood velocity, volume, and flow along with an increased mean vascular resistance in moderate myopes with mean refractive errors of -5.5 D.

Conclusion

Although extensive studies have investigated myopia-related vascular changes from various aspects, it remains difficult to conclude whether the ocular blood supply is affected by myopia-induced eyeball stretching based on contradictory evidence. OCTA technique has remarkably boost vascular-related studies in myopic eyes because it provides non-invasive, dye-free, quick three-dimensional vascular maps. However, standardization in ocular magnification, layer segmentation, projection removal, etc., is required to rule out the potential confounding factors and reveal the actual effect of myopia on ocular vessels. The image quality of the deep retina, peripheral region and choroid are suboptimal at the current stage. Image acquisition and processing require further improvements to visualize and quantify those areas in a more promising way. Hemodynamic studies provide valuable information of the ocular blood circulation. A strict control of experimental settings and cautious interpretations should be practiced when analyzing the effects of myopia on hemodynamic parameters due to the great individual differences and physiological fluctuations. Integrating isolated findings through multi-module imaging could help to decode the complexity of ocular vasculature.

The causal relationship between axial elongation and impaired ocular vasculature remains uncertain and awaits answers from longitudinal studies.

References

1 Holden BA, Fricke TR, Wilson DA et al. Global Prevalence of Myopia and High Myopia and Temporal Trends from 2000 through 2050. *Ophthalmology* 2016; 123: 1036-1042.

2 Morgan IG, French AN, Ashby RS et al. The epidemics of myopia: Aetiology and prevention. *Progress in Retinal and Eye Research* 2018; 62: 134-149.

3 Luong TQ, Shu Y-H, Modjtahedi BS et al. Racial and Ethnic Differences in Myopia Progression in a Large, Diverse Cohort of Pediatric Patients. *Investigative Ophthalmology & Visual Science* 2020; 61: 20-20.

4 Flitcroft DI, He M, Jonas JB et al. IMI - Defining and Classifying Myopia: A Proposed Set of Standards for Clinical and Epidemiologic Studies. *Invest Ophthalmol Vis Sci* 2019; 60: M20-M30.

5 Ohno-Matsui K, Wu P-C, Yamashiro K et al. IMI Pathologic Myopia. *Investigative Ophthalmology & Visual Science* 2021; 62: 5-5.

6 Wong CW, Yanagi Y, Tsai ASH et al. Correlation of axial length and myopic macular degeneration to levels of molecular factors in the aqueous. *Scientific Reports* 2019; 9: 15708.

7 Rong SS, Chen LJ, Pang CP. Myopia Genetics-The Asia-Pacific Perspective. *Asia Pac J Ophthalmol (Phila)* 2016; 5: 236-244.

8 Leveziel N, Yu Y, Reynolds R et al. Genetic factors for choroidal neovascularization associated with high myopia. *Invest Ophthalmol Vis Sci* 2012; 53: 5004-5009.

9 Guggenheim JA, Mojarrad N, Williams C et al. Genetic prediction of myopia: prospects and challenges. *Ophthalmic and Physiological Optics* 2017; 37: 549-556.

10 Wu H, Chen W, Zhao F et al. Scleral hypoxia is a target for myopia control. *Proc Natl Acad Sci U S A* 2018; 115: E7091-e7100.

11 Zhao F, Zhang D, Zhou Q et al. Scleral HIF-1α is a prominent regulatory candidate for genetic and environmental interactions in human myopia pathogenesis. *EBioMedicine* 2020; 57: 102878.

12 Corvi F, Pellegrini M, Erba S et al. Reproducibility of Vessel Density, Fractal Dimension, and Foveal Avascular Zone Using 7 Different Optical Coherence Tomography Angiography Devices. *American Journal of Ophthalmology* 2018; 186: 25-31.

13 Campbell JP, Zhang M, Hwang TS et al. Detailed Vascular Anatomy of the Human Retina by Projection-Resolved Optical Coherence Tomography Angiography. *Scientific Reports* 2017; 7: 42201.

14 Al-Sheikh M, Phasukkijwatana N, Dolz-Marco R et al. Quantitative OCT angiography of the retinal microvasculature and the choriocapillaris in myopic eyes. *Investigative Ophthalmology & Visual Science* 2017; 58: 2063-2069.

15 Fan H, Chen HY, Ma HJ et al. Reduced macular vascular density in myopic eyes. *Chinese Medical Journal* 2017; 130: 445-451.

16 Mo J, Duan A, Chan S et al. Vascular flow density in pathological myopia: an optical coherence tomography angiography study. *BMJ Open* 2017; 7: e013571.

17 Elsherif W, Moustafa M, Attaallah H et al. Macular microvaculature evaluation using optical coherence tomography angiography in patients with high myopia. *Egyptian Retina Journal* 2019; 6: 43-51.

18 Yang DW, Cao D, Zhang L et al. Macular and peripapillary vessel density in myopic eyes of young Chinese adults. *Clinical and Experimental Optometry* 2020; 103: 830-837.

19 Wen C, Pei C, Xu X et al. Influence of Axial Length on Parafoveal and Peripapillary Metrics from Swept Source Optical Coherence Tomography Angiography. *Curr Eye Res* 2019; 44: 980-986.

20 He J, Chen Q, Yin Y et al. Association between retinal microvasculature and optic disc alterations in high myopia. *Eye* 2019; 33: 1494-1503.

21 Min CH, Al-Qattan HM, Lee JY et al. Macular Microvasculature in High Myopia without Pathologic Changes: An Optical Coherence Tomography Angiography Study. *Korean J Ophthalmol* 2020; 34: 106-112.

22 Su L, Ji Y-S, Tong N et al. Quantitative assessment of the retinal microvasculature and choriocapillaris in myopic patients using swept-source optical coherence tomography angiography. *Graefes Arch Clin Exp Ophthalmol* 2020; 258: 1173-1180.

23 Ucak T, Icel E, Yilmaz H et al. Alterations in optical coherence tomography angiography findings in patients with high myopia. *Eye* 2020; 34: 1129-1135.

24 Zhu Q, Xing X, Wang M et al. Characterization of the Three Distinct Retinal Capillary Plexuses Using Optical Coherence Tomography Angiography in Myopic Eyes. *Transl Vis Sci Techn* 2020; 9: 8-8.

25 Yang Y, Wang J, Jiang H et al. Retinal microvasculature alteration in high myopia. *Investigative Ophthalmology & Visual Science* 2016; 57: 6020-6030.

26 Li M, Yang Y, Jiang H et al. Retinal microvascular network and microcirculation assessments in high myopia. *American Journal of Ophthalmology* 2017; 174: 56-67.

27 Liu M, Wang P, Hu X et al. Myopia-related stepwise and quadrant retinal microvascular alteration and its correlation with axial length. *Eye* 2020; 35: 2196-2205.

28 Sung MS, Lee TH, Heo H et al. Association Between Optic Nerve Head Deformation and Retinal Microvasculature in High Myopia. *American Journal of Ophthalmology* 2018; 188: 81-90.

29 Wang X, Kong X, Jiang C et al. Is the peripapillary retinal perfusion related to myopia in healthy eyes? a prospective comparative study. *BMJ Open* 2016; 6: e010791.

30 Yang SQ, Zhou MW, Lu B et al. Quantification of macular vascular density using optical coherence tomography angiography and its relationship with retinal thickness in myopic eyes of young adults. *Journal of Ophthalmology* 2017; 2017: 1397179.

31 Venkatesh R, Sinha S, Gangadharaiah D et al. Retinal structural-vascular-functional relationship using optical coherence tomography and optical coherence tomography – angiography in myopia. *Eye and Vision* 2019; 6: 8.

32 Guo Y, Sung MS, Park SW. Assessment of superficial retinal microvascular density in healthy myopia. *Int Ophthalmol* 2019; 39: 1861-1870.

33 Tan CS, Lim LW, Chow VS et al. Optical Coherence Tomography Angiography Evaluation of the Parafoveal Vasculature and Its Relationship With Ocular Factors. *Investigative Ophthalmology & Visual Science* 2016; 57: OCT224-234.

34 Ye J, Wang MY, Shen MX et al. Deep Retinal Capillary Plexus Decreasing Correlated With the Outer Retinal Layer Alteration and Visual Acuity Impairment in Pathological Myopia. *Investigative Ophthalmology & Visual Science* 2020; 61: 10.

35 Sampson DM, Gong P, An D et al. Axial Length Variation Impacts on Superficial Retinal Vessel Density and Foveal Avascular Zone Area Measurements Using Optical Coherence Tomography Angiography. *Investigative Ophthalmology & Visual Science* 2017; 58: 3065-3072.

36 MURDOCH IE, MORRIS SS, COUSENS SN. People and eyes: statistical approaches in ophthalmology. *British Journal of Ophthalmology* 1998; 82: 971-973.

37 Leng Y, Tam EK, Falavarjani KG et al. Effect of Age and Myopia on Retinal Microvasculature. *Ophthalmic Surg Lasers Imaging Retina* 2018; 49: 925-931.

38 Gómez-Ulla F, Cutrin P, Santos P et al. Age and gender influence on foveal avascular zone in healthy eyes. *Exp Eye Res* 2019; 189: 107856.

39 Milani P, Montesano G, Rossetti L et al. Vessel density, retinal thickness, and choriocapillaris vascular flow in myopic eyes on OCT angiography. *Graefes Arch Clin Exp Ophthalmol* 2018; 256: 1419-1427.

40 Lee K, Maeng KJ, Kim JY et al. Diagnostic ability of vessel density measured by spectral-domain optical coherence tomography angiography for glaucoma in patients with high myopia. *Scientific Reports* 2020; 10: 3027.

41 Zhu X, Meng J, Wei L et al. Cilioretinal Arteries and Macular Vasculature in Highly Myopic Eyes: An OCT Angiography-Based Study. *Ophthalmology Retina* 2020; 4: 965-972.

42 Meng J, Wei L, Zhang K et al. Cilioretinal Arteries in Highly Myopic Eyes: A Photographic Classification System and Its Association With Myopic Macular Degeneration. *Frontiers in Medicine* 2020; 7.

43 Gupta P, Thakku SG, Saw SM et al. Characterization of choroidal morphologic and vascular features in young men with high myopia using spectral-domain optical coherence tomography. *American Journal of Ophthalmology* 2017; 177: 27-33.

44 Alshareef RA, Khuthaila MK, Goud A et al. Subfoveal choroidal vascularity in myopia: evidence from spectral-domain optical coherence tomography. *Ophthalmic Surgery, Lasers & Imaging Retina* 2017; 48: 202-207.

45 Agrawal R, Gupta P, Tan K-A et al. Choroidal vascularity index as a measure of vascular status of the choroid: measurements in healthy eyes from a population-based study. *Scientific reports* 2016; 6: 21090.

46 Agrawal R, Wei X, Goud A et al. Influence of scanning area on choroidal vascularity index measurement using optical coherence tomography. *Acta ophthalmologica* 2017; 95: e770-e775.

47 Diaz JD, Wang JC, Oellers P et al. Imaging the Deep Choroidal Vasculature Using Spectral Domain and Swept Source Optical Coherence Tomography Angiography. *J Vitreoretin Dis* 2018; 2: 146-154.

48 Zhang Q, Zheng F, Motulsky EH et al. A novel strategy for quantifying choriocapillaris flow voids using swept-source OCT angiography. *Investigative ophthalmology & visual science* 2018; 59: 203-211.

49 Olver JM. Functional anatomy of the choroidal circulation: methyl methacrylate casting of human choroid. *Eye (Lond)* 1990; 4 (Pt 2): 262-272.

50 Li X-X, Wu W, Zhou H et al. A quantitative comparison of five optical coherence tomography angiography systems in clinical performance. *International journal of ophthalmology* 2018; 11: 1784.

51 Wong CW, Teo YCK, Tsai STA et al. Characterization of the Choroidal Vasculature in Myopic Maculopathy with Optical Coherence Tomographic Angiography. *Retina* 2018.

52 Sayanagi K, Ikuno Y, Uematsu S et al. Features of the choriocapillaris in myopic maculopathy identified by optical coherence tomography angiography. *British Journal of Ophthalmology* 2017; 101: 1524-1529.

53 Scherm P, Pettenkofer M, Maier M et al. Choriocapillary Blood Flow in Myopic Subjects Measured With OCT Angiography. *Ophthalmic Surg Lasers Imaging Retina* 2019; 50: e133-e139.

54 Spaide RF. Choriocapillaris flow features follow a power law distribution: implications for characterization and mechanisms of disease progression. *American Journal of Ophthalmology* 2016; 170: 58-67.

55 Borrelli E, Souied EH, Freund KB et al. Reduced Choriocapillaris Flow in Eyes with Type 3 Neovascularization and Age-Related Macular Degeneration. *Retina* 2018; 38: 1968-1976.

56 Zhang QQ, Shi YY, Zhou H et al. Accurate estimation of choriocapillaris flow deficits beyond normal intercapillary spacing with swept source OCT angiography. *Quant Imag Med Surg* 2018; 8: 658-666.

57 Mastropasqua R, Viggiano P, Borrelli E et al. In Vivo Mapping of the Choriocapillaris in High myopia: a Widefield Swept Source Optical Coherence Tomography Angiography. *Scientific Reports* 2019; 9: 18932.

58 Zhao J, Wang YX, Zhang Q et al. Macular Choroidal Small-Vessel Layer, Sattler's Layer and Haller's Layer Thicknesses: The Beijing Eye Study. *Sci Rep* 2018; 8: 4411.

59 Maruko I, Spaide RF, Koizumi H et al. Choroidal Blood Flow Visualization in High Myopia Using a Projection Artifact Method in Optical Coherence Tomography Angiography. *Retina* 2017; 37: 460-465.

60 Devarajan K, Sim R, Chua J et al. Optical coherence tomography angiography for the assessment of choroidal vasculature in high myopia. *British Journal of Ophthalmology* 2020; 104: 917-923.

61 Spaide RF, Klancnik JM, Jr., Cooney MJ. Retinal vascular layers imaged by fluorescein angiography and optical coherence tomography angiography. *JAMA Ophthalmol* 2015; 133: 45-50.

62 Chen Q, He J, Hua Y et al. Exploration of peripapillary vessel density in highly myopic eyes with peripapillary intrachoroidal cavitation and its relationship with ocular parameters using optical coherence tomography angiography. *Clinical & Experimental Ophthalmology* 2017; 45: 884-893.

63 Shin JW, Kwon J, Lee J et al. Choroidal Microvasculature Dropout is Not Associated With Myopia, But is Associated With Glaucoma. *J Glaucoma* 2018; 27: 189-196.

64 Comune C, Montorio D, Cennamo G. Optical coherence tomography angiography in myopic peripapillary intrachoroidal cavitation complicated by choroidal neovascularization. *European Journal of Ophthalmology* 2020: 5.

65 Lee SH, Lee EJ, Kim T-W. Comparison of vascular–function and structure–function correlations in glaucomatous eyes with high myopia. *British Journal of Ophthalmology* 2020; 104: 807-812.

66 Na H-M, Lee EJ, Lee SH et al. Evaluation of Peripapillary Choroidal Microvasculature to Detect Glaucomatous Damage in Eyes With High Myopia. *Journal of Glaucoma* 2020; 29: 39-45.

67 Kim GN, Lee EJ, Kim TW. Microstructure of Nonjuxtapapillary Microvasculature Dropout in Healthy Myopic Eyes. *Investigative Ophthalmology & Visual Science* 2020; 61: 8.

68 Kaneko Y, Moriyama M, Hirahara S et al. Areas of nonperfusion in peripheral retina of eyes with pathologic myopia detected by ultra-widefield fluorescein angiography. *Investigative Ophthalmology & Visual Science* 2014; 55: 1432-1439.

69 Quaranta M, Arnold J, Coscas G et al. Indocyanine Green Angiographic Features of Pathologic Myopia. *American Journal of Ophthalmology* 1996; 122: 663-671.

70 Moriyama M, Ohno-Matsui K, Futagami S et al. Morphology and long-term changes of choroidal vascular structure in highly myopic eyes with and without posterior staphyloma. *Ophthalmology* 2007; 114: 1755-1762.

71 OhnoMatsui K, Morishima N, Ito M et al. Posterior routes of choroidal blood outflow in high myopia. *Retina-J Ret Vit Dis* 1996; 16: 419-425.

72 Akyol N, Kukner AS, Ozdemir T et al. Choroidal and retinal blood flow changes in degenerative myopia. *Canadian Journal of Ophthalmology* 1996; 31: 113-119.

73 Benavente-Perez A, Hosking SL, Logan NS et al. Ocular blood flow measurements in healthy human myopic eyes. *Graefes Archive for Clinical & Experimental Ophthalmology* 2010; 248: 1587-1594.

74 Karczewicz D, Modrzejewska M. [Blood flow in eye arteries assessed by Doppler ultrasound in patients with myopia]. *Klinika Oczna* 2004; 106: 211-213.

75 Montanari P, Marangoni P, Pinotti D et al. High myopia and glaucoma: color Doppler imaging of the optic nerve vasculature. *Acta Ophthalmol Scand* 1999; 77: 42-43.

76 Mrugacz M, Bryl A. [Evaluation of the arterial blood flow parameters in the eye of myopic patients]. *Polski Merkuriusz Lekarski* 2013; 34: 205-209.

77 Galassi F, Sodi A, Ucci F et al. Ocular haemodynamics in glaucoma associated with high myopia. *International ophthalmology* 1998; 22: 299-305.

78 Dimitrova G, Tamaki Y, Kato S et al. Retrobulbar circulation in myopic patients with or without myopic choroidal neovascularisation. *British Journal of Ophthalmology* 2002; 86: 771-773.

79 Stalmans I, Vandewalle E, Anderson DR et al. Use of colour Doppler imaging in ocular blood flow research. *Acta Opthalmologica* 2011; 89: e609-630.

80 Silver DM, Geyer O. Pressure-volume relation for the living human eye. *Current Eye Research* 2000; 20: 115-120.

81 Mori F, Konno S, Hikichi T et al. Factors affecting pulsatile ocular blood flow in normal subjects. *British Journal of Ophthalmology* 2001; 85: 529-530.

82 Lam AKC, Wong S, Lam CSY et al. The effect of myopic axial elongation and posture on the pulsatile ocular blood flow in young normal subjects. *Optometry and Vision Science* 2002; 79: 300-305.

83 Berisha F, Findl O, Lasta M et al. A study comparing ocular pressure pulse and ocular fundus pulse in dependence of axial eye length and ocular volume. *Acta ophthalmologica* 2010; 88: 766-772.

84 Dastiridou AI, Ginis H, Tsilimbaris M et al. Ocular Rigidity, Ocular Pulse Amplitude, and Pulsatile Ocular Blood Flow: The Effect of Axial Length. *Investigative Ophthalmology & Visual Science* 2013; 54: 2087-2092.

85 Yang YS, Koh JW. Choroidal Blood Flow Change in Eyes with High Myopia. *Korean Journal of Ophthalmology* 2015; 29: 309-314.

86 Dastiridou AI, Ginis HS, De Brouwere D et al. Ocular Rigidity, Ocular Pulse Amplitude, and Pulsatile Ocular Blood Flow: The Effect of Intraocular Pressure. *Investigative Ophthalmology & Visual Science* 2009; 50: 5718-5722.

87 Shimada N, Ohno-Matsui K, Harino S et al. Reduction of retinal blood flow in high myopia. *Graefes Archive for Clinical & Experimental Ophthalmology* 2004; 242: 284-288.

88 Zheng Q, Zong Y, Li L et al. Retinal vessel oxygen saturation and vessel diameter in high myopia. *Ophthalmic & Physiological Optics* 2015; 35: 562-569.

89 La Spina C, Corvi F, Bandello F et al. Static characteristics and dynamic functionality of retinal vessels in longer eyes with or without pathologic myopia. *Graefes Archive for Clinical & Experimental Ophthalmology* 2016; 254: 827-834.

90 Li H, Mitchell P, Rochtchina E et al. Retinal Vessel Caliber and Myopic Retinopathy: The Blue Mountains Eye Study. *Ophthalmic Epidemiol* 2011; 18: 275-280.

91 Chen HC, Patel V, Wiek J et al. Vessel Diameter Changes during the Cardiac Cycle. *Eye* 1994; 8: 97-103.

92 Hao H, Sasongko MB, Wong TY et al. Does retinal vascular geometry vary with cardiac cycle? *Invest Ophthalmol Vis Sci* 2012; 53: 5799-5805.

93 Streese L, Brawand LY, Gugleta K et al. New Frontiers in Noninvasive Analysis of Retinal Wall-to-Lumen Ratio by Retinal Vessel Wall Analysis. *Transl Vis Sci Techn* 2020; 9: 7-7.

94 Heitmar R. Retinal Vessel Oxygen Saturation and its implications in myopia. *Acta ophthalmologica* 2015; 93.

95 Lim LS, Lim XH, Tan L. Retinal Vascular Oxygen Saturation and Its Variation With Refractive Error and Axial Length. *Transl Vis Sci Techn* 2019; 8.

96 Neriyanuri S, Bedggood PA, Symons RCA et al. Characterizing spatial and temporal heterogeneity in retinal capillary blood flow. *Investigative Ophthalmology & Visual Science* 2019; 60: 4596-4596.

97 Qu D, Lin Y, Jiang H et al. Retinal nerve fiber layer (RNFL) integrity and its relations to retinal microvasculature and microcirculation in myopic eyes. *Eye and Vision* 2018; 5: 25.

98 Benavente-Perez A, Hosking SL, Logan NS. Myopes Exhibit Reduced Choroidal Blood Velocity Which Is Highly Responsive to Hypercapnia. *Investigative Ophthalmology & Visual Science* 2008; 49: 3581-3581.

99 Samra WA, Pournaras C, Riva C et al. Choroidal hemodynamic in myopic patients with and without primary open-angle glaucoma. *Acta ophthalmologica* 2013; 91: 371-375.

TABLE 1 A summary of myopia-related OCTA studies in the macular area published in the recent 5 years.

Study	Subjects						Measurements				Major findings		
	No. (e)	No. (s)	Group (Definition)	Age (years)	AL (mm)	SE (diopter)	Device (Protocol)	Layer segmentation	Image processing	Magnification correction	SCP	DCP	Other layers
Tan, et al. [33] (2016)	56	117	**HM** (SE < -6 D, no myopic complications)	22.5 ± 1.4	25.4 ± 1.3	-4.3 ± 2.9	RTVue 3 × 3 mm	SCP: ILM-3 to IPL-15 μm DCP: IPL-15 to IPL-69 μm	ImageJ	Unknown	AL was a negative predictor of FAZ area in HM	Same as SCP	NA
	178		**MIM / EM**										
Wang, et al. [29] (2016)	18	18	**HM** (SE ≤ −6.0 D)	16.3 ± 0.5	26.6 ± 0.9	-8.0 ± 0.8	RTVue 3 × 3 mm	SCP: ILM-3 to IPL-29 μm cc: RPE-29 to RPE-59 μm	AngioVue	Unknown	No significant group difference in VAD or flow index	NA	**cc**: No significant group difference in VAD or flow index
	20	20	**MOM** (SE: -5.75 to -3.00 D)	16.8 ± 0.8	25.7 ± 0.8	-4.6 ± 0.8							
	20	20	**MIM** (SE: -2.75 to -0.75 D)	16.8 ± 0.7	24.2 ± 0.8	-1.7 ± 0.6							
	20	20	**EM** (SE: -0.50 to +0.50 D)	16.6 ± 0.9	23.9 ± 0.6	-0.1 ± 0.4							
Yang, et al. [25] (2016)	33	21	**HM** (SE < -6.00 D)	26.0 ± 2.7	27.1 ± 1.3	-8.7 ± 1.9	RTVue 3 × 3 mm	SCP: ILM-3 to IPL-15 μm DCP: IPL-15 to IPL-69 μm	Matlab program	Yes (resize)	Decreased FD in HM; negative correlations between FD and AL	Same as SCP	NA
	47	24	**MIM / EM** (SE: -3.00 to +0.50 D)	27.4 ± 6.4	23.8 ± 0.8	-0.8 ± 1.0							
Al-Sheikh, et al. [14] (2017)	50	28	**HM** (Refraction < −6.00 D or AL > 26.5 mm, exclude diffuse RPE atrophy)	57.0 ± 17.9	-	-8.3 ± 2.9	RTVue 3 × 3 mm	SCP: ILM-3 to IPL-15 μm DCP: IPL-15 to IPL-70 μm cc: RPE-34 to RPE-44 μm	FIJI	Unknown	Decreased VAD and FD in HM	Same as superficial	Total number of flow void: HM < control Total and average area of flow void: HM > control
	34	20	**Control** (Refraction > −2.50 D)	56.1 ± 19.3	-	0.0 ± 1.1							
Fan, et al. [15] (2017)	30	47	**HM** (SE ≤ −6.00 D)	36.3 ± 14.7	29.0 ± 2.7	−11.6 ± 5.4	RTVue 3 × 3 mm	SCP: ILM-3 to IPL-15 μm* DCP: IPL-15 to IPL-69 μm*	ImageJ	Unknown	VAD: HM, MOM > control; VAD negatively associated with AL, and positively with SE and mGCC thickness	VAD: HM > control; VAD negatively associated with AL, and positively with SE and GCC thickness	NA
	33		**MOM** (-6.00 D < SE ≤ −3.00 D)	30.9 ± 4.1	25.0 ± 0.5	-3.8 ± 1.3							
	28		**Control** (SE < 3.00 D and SE > -3.00 D)	34.1 ± 15.8	23.3 ± 0.5	-0.7 ± 0.7							
Li, et al. [26] (2017)	20	20	**HM** (SE < −5 D, non-pathological)	28.0 ± 5.0	26.4 ± 1.0	−6.3 ± 1.2	Cirrus 3 × 3 mm	SCP: ILM to IPL DCP: INL to OPL	Matlab program	Yes (resize)	Decreased microvascular FD in HM; negative correlation between FD and AL	Decreased microvascular FD in myopia; FD showed negative correlation with AL	NA
	20	20	**Control** (SE > −3 D)	30.0 ± 6.0	24.1 ± 1.0	−1.4 ± 1.0							
Mo, et al. [16] (2017)	45	-	**PM** (SE ≤−6.00 D and AL>26.5 mm, with pathological changes)	38.0 ± 11.7	29.6 ± 1.7	−15.2 ± 3.8	RTVue 3 × 3 mm	SCP: ILM-3 to IPL-16 μm DCP: IPL-16 to IPL-69 μm cc: RPE-31 to RPE-59μm	AngioVue	Unknown	VAD: PM < HM/EM negative correlation between AL and superficial VAD; positive correlation between BCVA and superficial VAD	Same as superficial	VAD: HM/PM < EM
	41	-	**HM** (SE ≤−6.00 D, without pathological changes)	33.3 ± 15.0	25.9 ± 0.6	−6.9 ± 1.2							
	45	-	**EM** (SE: -0.50 to +0.50 D)	38.3 ± 13.1	23.2 ± 0.6	0.1 ± 0.4							
Yang, et al. [30] (2017)	70	145	**HM** (SE < −6.00 D)	26.1 ± 1.7	26.2 ± 0.9	−7.1 ± 0.9	RTVue 3 × 3 mm	SCP: ILM-3 to IPL-15 μm DCP: IPL-15 to IPL-70 μm	AngioVue	Unknown	No difference in VAD among 3 groups VAD showed negative correlation with mean arterial pressure, positive correlation with mGCC thickness	No difference in VAD among 3 groups VAD showed negative correlation with mean arterial pressure, positive correlation with retinal thickness	NA
	117		**MOM** (−3.00 D < SE ≤ −6.00 D)	26.0 ± 1.6	25.2 ± 0.8	−4.7 ± 0.8							
	81		**MIM** (−0.50 D < SE ≤ −3.00 D)	26.1 ± 2.0	24.2 ± 0.9	−1.8 ± 0.7							

Milani, et al. [39] (2018)	42	37	**HM** (SE ≤ −6.00D, exclude chorioretinal and RPE atrophy)	51.9 ± 10.9	-	-10.3 ± 3.8	RTVue 3 × 3 mm	SCP: ILM-3 to IPL-16 μm ORL: IPL-72μm to RPE-31μm cc: RPE-31 to RPE-59μm	AngioVue	Unknown	VAD: HM < control	NA	**ORL:** higher flow area (mm^2) in HM **cc:** no significant group difference
	40	28	**Control** (SE 0 ± 2D)	56.2 ± 16.6	-	-0.1 ± 1.4							
Sung, et al. [28] (2018)	71	71	**HM** (AL between 26 to 28 mm, exclude pathological myopia)	23.6 ± 4.0	26.7 ± 0.6	-7.4 ± 1.7	RTVue 3 × 3 mm	SCP: ILM-3 to IPL-15 μm DCP: IPL-15 to IPL-70 μm	AngioVue	Yes (only for FAZ)	Enlarged superficial FAZ	Enlarged deep FAZ	NA
	26	26	**EM** (SE between -0.5 to +0.5D, and AL between 22 to 24mm)	23.1 ± 4.3	23.5 ± 0.6	-0.1 ± 0.4							
Elsherif, et al. [17] (2019)	50	30	**HM** (SE < -6 D and AL > 25.5 mm)	33.9 ± 7.3	27.6 ± 1.9	−10.5 ± 2.9	RTVue 6 × 6 mm	SCP: ILM-3 to IPL-15 μm* DCP: IPL-15 to IPL-70 μm*	AngioVue	Unknown	Reduced overall and foveal VAD in HM, but parafoveal VAD was comparable in two groups	Same as SCP	NA
	25	25	**Control**	33.8 ± 4.9	22.7 ± 0.5	0.1 ± 0.7							
Guo, et al. [32] (2019)	45	45	**HM** (SE < -6.00 D)	23.6 ± 3.8	27.1 ± 1.0	- 8.6 ± 1.7	RTVue 3 × 3 mm	SCP: ILM-3 to IPL-15 μm	AngioVue	Unknown	No significant difference in VAD among four groups	NA	NA
	76	76	**MOM** (−6.00 D ≤ SE < −3.00 D)	23.6 ± 3.8	25.9 ± 0.9	- 4.7 ± 0.9							
	32	32	**MIM** (−3.00 D ≤ SE < -1.00 D)	24.1 ± 4.1	24.9 ± 0.8	- 2.3 ± 0.8							
	21	21	**EM** (−1.00 D ≤ SE < +0.75 D)	21.9 ± 2.9	23.6 ± 1.2	- 0.8 ± 0.3							
He, et al. [20] (2019)	221	221	**HM** (AL ≥ 26 mm)	20.0 ± 2.6	26.4 ± 1.1	−5.8 ± 3.0	RTVue 6 × 6 mm	SCP: ILM-3 to IPL-15 μm DCP: IPL-15 to IPL-70 μm	AngioVue	Yes (only for FAZ)	AL was significant negative predictor of VAD and FAZ No group difference in VAD Enlarged FAZ in HM (> MIM/EM)	VAD: EM/MIM > MOM > HM AL was significant negative predictor of VAD	NA
	243	243	**MOM** (AL: 25 to 26 mm)	19.8 ± 2.4	25.4 ± 0.5	−4.4 ± 2.0							
	211	211	**MIM** (AL: 24 and 25 mm)	19.9 ± 3.0	24.5 ± 0.3	−2.9 ± 1.8							
	85	85	**EM** (AL: 23 and 24 mm)	20.2 ± 2.5	23.6 ± 0.3	−1.8 ± 1.5							
Mastropasqua, et al. [57] (2019)	30	30	**HM** (AL > 26.5 mm, without any structural changes. e.g. dome-shaped retina, mCNV, staphyloma)	26.9 ± 2.9	26.6 ± 0.6	-	PLEX Elite 9000 Five 12 × 12-mm scan	cc: RPE-29 to RPE-49μm*	ImageJ	Unknown	NA	NA	Total flow void area was greater in HM than control in macular, paramacular regions
	50	50	**Control**	25.2 ± 5.1	23.9 ± 1.1	-							
Scherm, et al. [53] (2019)	78	45	**Myopia** (SE between -1 to -6D, AL between 20 to 26.5 mm)	29.3 ± 5.0	24.3 ± 1.0	-2.6 ± 1.4	RTVue 3 × 3 mm	cc: RPE-31 to RPE-60 μm	AngioVue	Unknown	NA	NA	**cc:** no significant group difference in flow area; no correlation between AL and flow area
	79	44	**EM** (SE between -0.75 to +0.75 D)	28.6 ± 5.1	23.5 ± 0.8	-0.2 ± 0.4							
Venkatesh, et al. [31] (2019)	86	54	**Healthy**	33.3 ± 14.5	26.0 ± 2.4	-7.2 ± 5.7	RTVue 3 × 3 mm	SCP: ILM-3 to IPL-15 μm DCP: IPL-16 to IPL-69 μm	AngioVue	Unknown	No significant correlation between AL and VAD/ flow index	VAD was positively correlated with AL; no correlation between AL and flow index	NA
Wen, et al. [19] (2019)	75	75	**Healthy** (exclude myopic maculopathy other than tessellated fundus)	26.6 ± 6.8	24.9± 1.3	-	Triton 3 × 3 mm	SCP: ILM-2.6 to IPL-15.6 μm	ImageJ	Yes (resize)	AL was a negative predictor for VAD and VLD No correlation between AL and FAZ area	NA	NA
	28	28	**Extreme HM** (SE ≤ −10.0 D)	25.9 ± 5.4	28.4 ± 1.1	−12.4 ± 2.5	Cirrus	SCP: ILM to IPL		Yes (resize)		Same as SCP	NA

Liu, et al. [27] (2020)	86	86	**HM** (−10.0 D < SE ≤ −6.0 D)	24.2 ± 5.6	26.7 + 0.9	−7.6 ± 2.7	6 × 6 mm	DCP: INL to OPL	Matlab program		FD: MIM > MOM > HM > extreme HM; FD negatively correlated with AL		
	72	72	**MOM** (−6.0 D < SE ≤ −3.0 D)	23.5 ± 5.1	25.7 ± 0.8	−4.8 ± 0.8							
	22	22	**MIM** (−3.0 D < SE ≤ −0.5 D)	23.8 ± 8.4	24.9 ± 0.8	−2.2 ± 0.6							
Min, et al. [21] (2020)	52	52	**HM** (AL > 26.5 mm, no pathological changes)	45.7 ± 15.0	27.5 ± 1.1	-8.5 ± 4.9	RTVue 3 × 3 mm	SCP: ILM-3 to IPL-15 μm* DCP: IPL-15 to IPL-70 μm*	AngioVue	Yes (only for FAZ)	FAZ: HM > control VAD: HM < control	VAD: no group difference	NA
	52	52	**Control** (AL < 26.5 mm)	46.5 ± 16.6	24.0 ± 1.1	-2.0 ± 3.0							
Su, et al. [22] (2020)	25	25	**HM (**SE ≤ −6.0 D or AL ≥ 26.5 mm, excluded lacquer cracks or chorioretinal atrophy)	35.4 ± 12.4	27.6 ± 1.1	-7.5 ± 1.8	PLEX Elite 9000 6 × 6 mm	SCP: ILM to IPL DCP: INL to OPL cc: RPE-21 to RPE-31μm	ImageJ	Yes (resize)	VAD: HM < EM VLD: HM / MOM < EM	VAD: no group difference VLD: HM < MOM / EM	**cc**: flow void (%) of HM > MOM / EM
	25	25	**MOM** (-6.0 D < SE ≤ −3.0 D)	33.5 ± 8.9	25.3 ± 0.7	-4.1 ± 1.6							
	25	25	**MIM / EM** (SE > -3.0 D, no hyperopia)	35.0 ± 11.4	23.8 ± 0.8	-1.2 ± 1.0							
Ucak, et al. [23] (2020)	92	92	**HM** (AL ≥ 26 mm, excluded myopic maculopathy other than tessellated fundus)	35.2 ± 14.3	27.0 ± 0.8	−8.1 ± 1.7	Nidek RS3000 3 × 3 mm	SCP: ILM to IPL DCP: INL to OPL	AngioScan	Yes (calculation?)	FAZ: no group difference VAD: HM < control	Same as SCP	NA
	70	70	**Control**	36.2 ± 11.4	23.1 ± 0.8	0.5 ± 0.3							
Yang, et al. [18] (2020)	41	41	**HM** (SE ≤ −6.0 D, excluded pathological myopia)	21.3 ± 0.8	26.7 ± 0.9	−7.2 ± 1.2	RTVue 6 × 6 mm	SCP: ILM to IPL + 10 μm DCP: IPL + 10 to OPL-10 μm	AngioVue	No	VAD: HM < MIM Negative correlation between AL and VAD	Same as SCP	NA
	45	45	**MOM** (−6.0 D < SE ≤ −3.0 D)	20.8 ± 0.6	25.2 ± 0.7	−4.6 ± 0.8							
	42	42	**MIM** (−3.0 D < SE < −0.5 D)	21.8 ± 1.2	23.9 ± 0.5	−1.9 ± 0.6							
Ye, et al. [34] (2020)	22	22	**PM** (SE ≤ −6.00 D, or AL ≥ 26.5 mm, with myopic maculopathy)	37.7 ± 11.4	29.2 ±1.2	-13.9 ± 3.3	RTVue 3 × 3 mm	SCP: ILM to IPL + 10 μm DCP: IPL + 10 to OPL-10 μm	Custom-developed software	Yes (resize ?)	VAD: PM / HM < control Decreased VAD was correlated worse BCVA in PM and HM	VAD: PM < HM < control Decreased VAD was correlated worse BCVA in PM and HM	NA
	48	48	**HM** (SE ≤ −6.00D, or AL ≥ 26.5 mm, without myopic maculopathy)	32.4 ± 9.1	27.7 ±1.2	-10.3 ± 2.7							
	21	21	**Control** (SE between -1.0 to +1.0 D)	37.5 ± 13.6	24.1 ± 0.7	-0.51 ± 0.9							
Zhu, et al. [24] (2020)	25	62	**Super HM** (SE ≤ −9.00 D)	26.5 ± 6.9	27.3 ± 1.0	-10.2 ± 1.1	Cirrus 3 × 3 mm	SCP: ILM to ILM-70 μm MCP: 30-μm slab, near IPL DCP: 20-μm slab, near OPL *MCP and DCP were adjusted individually*	ImageJ	Yes (resize)	VAD: no group difference VLD: super HM / HM < control	VAD: super HM > MOM / control; HM > MOM / control	**MCP**: VAD: super HM > MOM / control; VLD: super HM / HM < control)
	57		**HM** (−9.00D < SE ≤ −6.00 D)	27.6 ± 6.4	26.7 ± 1.2	-7.4 ± 0.8							
	14		**MOM** (−6.00D < SE ≤ −3.00 D)	29.9 ± 8.2	24.8 ± 0.7	-4.1 ± 0.8							
	30	15	**Control**	28.3 ± 3.1	23.3 ± 0.7	-0.2 ± 0.6							

No. (e), number of eyes; No. (s), number of subjects; PM, pathological myopia; HM, high myopia; MOM, moderate myopia; MIM, mild myopia; EM, emmetropia; AL, axial length; SE, spherical equivalent; SCP/DCP/MCP, superficial/deep/middle capillary plexus; ORL, outer retinal layer; cc, choriocapillaris; ILM, inner limiting membrane; IPL/OPL, inner/outer plexiform layer; RPE, retinal pigment epithelium; VAD, vessel area density; FD, fractal dimension; FAZ, foveal avascular zone; mGCC, macular ganglion cell complex

** default layer segmentation of OCTA device was illustrated here if not otherwise specified in the paper; "-"means below and "+" means above, e.g. ILM – 150μm means 150μm below the ILM layer.*

TABLE 2 A summary of myopia-related OCTA studies in the peripapillary area published in the recent 5 years.

Study	Subjects						Measurements			Major findings
	No. (e)	No. (s)	Group (Definition)	Age (years)	AL (mm)	SE (diopter)	Device (Protocol)	Layer segmentation	Image processing	
Wang, et al. [29] (2016)	18	18	**HM** (SE ≤ −6.0 D)	16.3 ± 0.5	26.6 ± 0.9	-8.0 ± 0.8	RTVue 4.5 × 4.5 mm	Retina: ILM to RPE Choroid: RPE to RPE-75μm*	AngioVue	**Retina:** VAD and flow index: HM < MIM / EM; negative correlation between the AL and flow index; positive correlation between RNFL thickness and VAD, flow index **Choroid:** no significant group differences in VAD or flow index
	20	20	**MOM** (SE: -5.75 to -3.00 D)	16.8 ± 0.8	25.7 ± 0.8	-4.6 ± 0.8				
	20	20	**MIM** (SE: -2.75 to -0.75 D)	16.8 ± 0.7	24.2 ± 0.8	-1.7 ± 0.6				
	20	20	**EM** (SE: -0.50 to +0.50 D)	16.6 ± 0.9	23.9 ± 0.6	-0.1 ± 0.4				
Chen, et al. [62] （2017）	35	35	**HM with PICC** (SE < -6 D or AL > 26.0 mm, PICC in OCT)	50.9 ± 12.5	28.5 ± 1.6	-11.5 ± 3.6	RTVue 4.5 × 4.5 mm	RPC: IML to RNFL ONH: ILM to ILM-150μm	AngioVue	**RPC:** VAD of HM with PICC < HM without PICC < Healthy; negative correlation between VAD and age, AL, PPA area; positive correlation between VAD and SE, RNFL thickness **ONH:** same as RPC
	46	46	**HM without PICC** (SE < -6 D or AL > 26.0 mm)	46.8 ± 14.4	28.1 ± 1.9	-9.7 ± 3.7				
	36	36	**Healthy**	49.2 ± 13.1	23.5 ± 0.9	0.1 ± 1.9				
Fan, et al. [15] (2017)	30	47	**HM** (SE≤−6.00 D)	36.3 ± 14.7	29.0 ± 2.7	−11.6 ± 5.4	RTVue 4.5 × 4.5 mm	ONH: ILM to ILM-150μm *	ImageJ	No significant group difference in VAD
	33		**MOM** (-6.00 D < SE≤−3.00 D)	30.9 ± 4.1	25.0 ± 0.5	-3.8 ± 1.3				
	28		**Control** (SE<3.00 D and SE>-3.00 D)	34.1 ± 15.8	23.3 ± 0.5	-0.7 ± 0.7				
Mo, et al. [16] (2017)	45	-	**PM** (SE ≤−6.00 D and AL>26.5 mm, with pathological changes)	38.0 ± 11.7	29.6 ± 1.7	−15.2 ± 3.8	RTVue 4.5 × 4.5 mm	RPC: IML to RNFL	AngioVue	VAD: PM < HM < EM; negative correlation between AL and VAD of RPC
	41	-	**HM** (SE ≤−6.00 D, without pathological changes)	33.3 ± 15.0	25.9 ± 0.6	−6.9 ± 1.2				
	45	-	**EM** (SE: -0.50 to +0.50 D)	38.3 ± 13.1	23.2 ± 0.6	0.1 ± 0.4				
Shin, et al. [63]	89	89	**Myopic OAG** (SE < -1.0 D, or AL > 24 mm, glaucoma)	47.0 ± 12.6	26.7 ± 1.4	−5.7 ± 3.4	RTVue 4.5 × 4.5 mm	RPC: IML to RNFL Choroid: RPE to RPE-75μm*	AngioVue	VAD: myopic OAG < Healthy control β PPA area: no significant difference between myopic OAG and healthy control % of CMvD: myopic OAG > Healthy control (40% vs 0)
	89	89	**Healthy control** (age- and refractive error-matched)	46.8 ± 12.8	26.5 ± 1.3	−5.5 ± 2.9				
Sung, et al. [28] (2018)	71	71	**HM** (AL between 26 to 28 mm, exclude pathological myopia)	23.6 ± 4.0	26.7 ± 0.6	-7.4 ± 1.7	RTVue 4.5 × 4.5 mm	RPC: IML to RNFL	AngioVue	VAD: HM < EM
	26	26	**EM** (SE between -0.5 to +0.5 D, and AL between 22 to 24 mm)	23.1 ± 4.3	23.5 ± 0.6	-0.1 ± 0.4				
Guo, et al. [32] (2019)	45	45	**HM** (SE < -6.00 D)	23.6 ± 3.8	27.1 ± 1.0	- 8.6 ± 1.7	RTVue 4.5 × 4.5 mm	RPC: IML to RNFL	AngioVue	VAD: HM < MOM/MIM/EM; positive correlation between VAD and RNFL thickness; negative correlation between VAD and AL
	76	76	**MOM** (−6.00 D≤ SE < −3.00 D)	23.6 ± 3.8	25.9 ± 0.9	- 4.7 ± 0.9				
	32	32	**MIM** (−3.00 D ≤ SE < -1.00 D)	24.1 ± 4.1	24.9 ± 0.8	- 2.3 ± 0.8				
	21	21	**EM** (−1.00 D ≤ SE < +0.75 D)	21.9 ± 2.9	23.6 ± 1.2	- 0.8 ± 0.3				
He, et al. [20] (2019)	221	221	**HM** (AL ≥ 26 mm)	20.0 ± 2.6	26.4 ± 1.1	−5.8 ± 3.0	RTVue 6 × 6 mm	RPC: IML to RNFL	AngioVue	VAD: HM/MOM < MIM/EM; negative correlation between VAD and AL, area of PPA; positive correlation between VAD and SE, RNFL thickness
	243	243	**MOM** (AL: 25 to 26 mm)	19.8 ± 2.4	25.4 ± 0.5	−4.4 ± 2.0				
	211	211	**MIM** (AL: 24 and 25 mm)	19.9 ± 3.0	24.5 ± 0.3	−2.9 ± 1.8				
	85	85	**EM** (AL: 23 and 24 mm)	20.2 ± 2.5	23.6 ± 0.3	−1.8 ± 1.5				

Wen, et al. [19] (2019)	75	75	**Healthy** (exclude myopic maculopathy other than tessellated fundus)	26.6 ± 6.8	24.9± 1.3	-	Triton 3 × 3 mm	ONH: ILM to ILM-150μm	ImageJ	No significant correlation between VAD, VLD and AL
Mastropasqua, et al. [57] (2019)	30	30	**HM** (AL > 26.5 mm, without any structural changes. e.g. dome-shaped retina, mCNV, staphyloma)	26.9 ± 2.9	26.6 ± 0.6	-	PLEX Elite 9000 Five 12 × 12-mm scan	cc: RPE-29 to RPE-49μm*	ImageJ	Total flow void area was greater in HM than control
	50	50	**Control**	25.2 ± 5.1	23.9 ± 1.1	-				
Comune, et al. [64] (2020)	12	12	**HM + PICC + CNV** (treatment-naïve)	66.9 ± 4.0	-	-9.5 ± 1.6	RTVue 4.5 × 4.5 mm	RPC: ILM to RNFL	AngioVue	VAD: (HM + PICC + CNV) < (HM + PICC) < HM
	21	21	**HM + PICC**	64.8 ± 6.0	-	-8.7 ± 1.9				
	23	23	**HM** (AL > 26 mm and SE < -6 D, with pathological changes)	65.5 ± 8.0	-	-9.3 ± 1.7				
Yang, et al. [18] (2020)	41	41	**HM** (SE ≤ −6.0 D, exclude pathological myopia)	21.3 ± 0.8	26.7 ± 0.9	−7.2 ± 1.2	RTVue 4.5 × 4.5 mm	RPC: ILM to RNFL	AngioVue	VAD: HM < MIM
	45	45	**MOM** (−6.0 D < SE ≤ −3.0 D)	20.8 ± 0.6	25.2 ± 0.7	−4.6 ± 0.8				
	42	42	**MIM** (−3.0 D < SE < −0.5 D)	21.8 ± 1.2	23.9 ± 0.5	−1.9 ± 0.6				

No. (e), number of eyes; No. (s), number of subjects; PM, pathological myopia; HM, high myopia; MOM, moderate myopia; MIM, mild myopia; EM, emmetropia; AL, axial length; SE, spherical equivalent; RPC, radial peripapillary capillary; ONH, optic nerve head; cc, choriocapillaris; ILM, inner limiting membrane; IPL/OPL, inner/outer plexiform layer; RPE, retinal pigment epithelium; RNFL, retinal nerve fiber layer; VAD, vessel area density; VLD, vessel length density; PPA, peripapillary atrophy; PICC, peripapillary intrachoroidal cavitation; CNV, choroidal neovascularization; OAG open-angle glaucoma; cMvD, choroidal microvascular dropout.

** default layer segmentation of OCTA device was illustrated here if not otherwise specified in the paper; "-"means below and "+" means above, e.g. ILM – 150μm means 150μm below the ILM layer.*

FIGURES

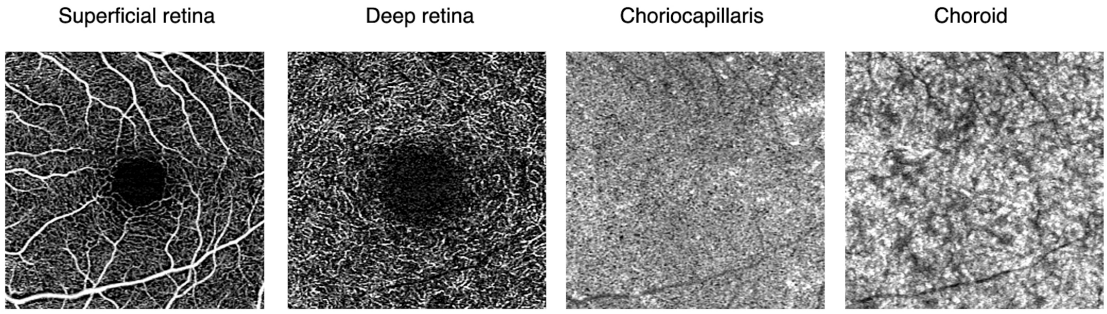

FIGURE 1 An example of OCTA angiogram of superficial retina, deep retina, choriocapillaris and choroid of a healthy young adult.

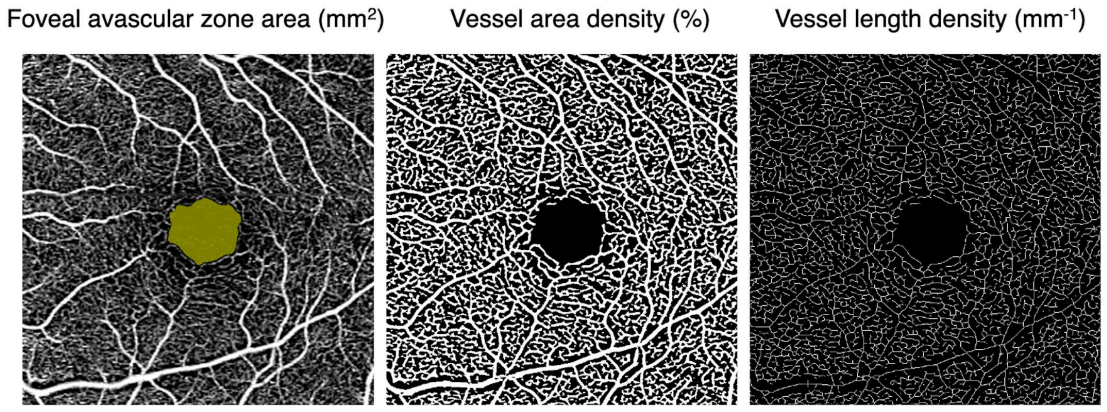

FIGURE 2 Calculation of foveal avascular zone (FAZ), vessel area density (VAD) and vessel length density (VLD). FAZ area (mm^2) is marked by the central yellow region in the left panel; VAD (%) is the percentage of white area (vessels) on background; VLD (mm^{-1}) is the ratio of vessel length (white branches in the right panel) on the background.

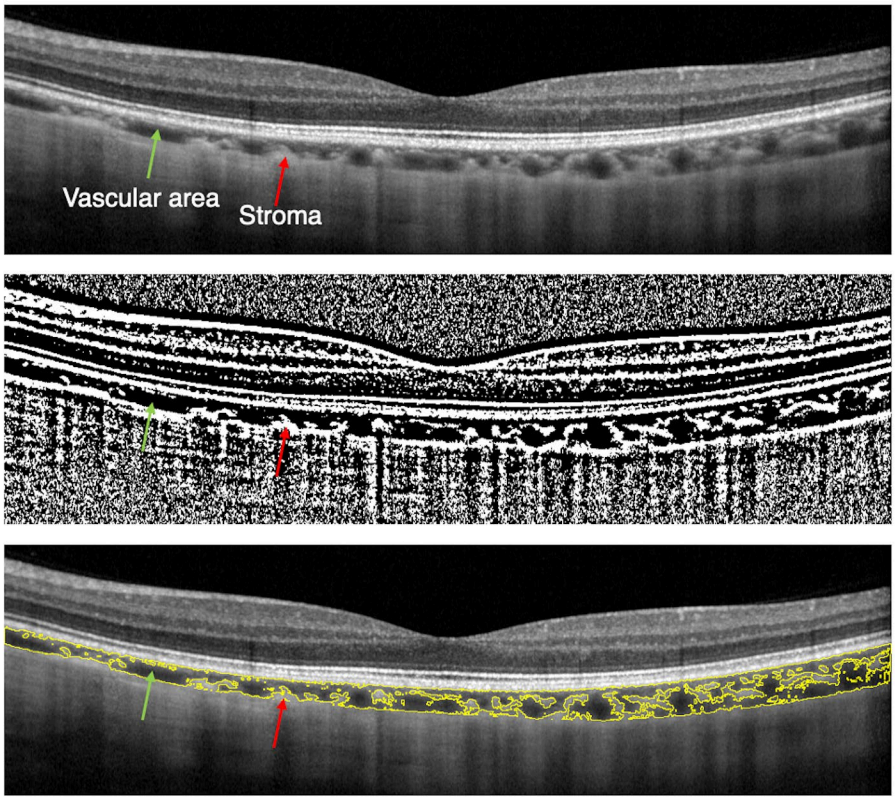

FIGURE 3 Choroidal vascularity index (CVI) obtained from the OCT B-scan. The raw image (top) is binarized (middle) to distinguish stroma from choroidal vessels, which is outlined and superimposed to the raw scan (bottom). The CVI is defined as the ratio of vascular regions relative to the overall choroidal area. The vascular area and stroma are indicated by green and red arrows, respectively.

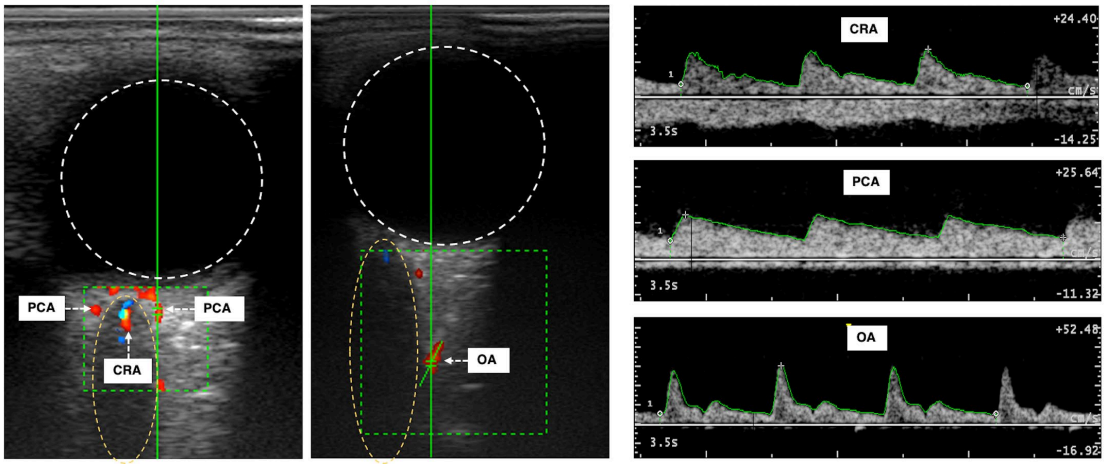

FIGURE 4 Measurement locations and waveforms of retrobulbar vessels in color doppler ultrasonography. The left panel illustrates the measurement locations of the central retinal artery (CRA) and posterior ciliary arteries (PCA). The approximate locations of eyeball and optic nerve are outlined by the white circle and the yellow ellipse, respectively. Blood

flow signals (blue and red) appear within the green rectangle. Similarly, the location of the ophthalmic artery (OA) is shown in the middle. Typical waveforms of three vessels are presented in the right panel.